Spin-glass behaviour in dilute weak random-anisotropy magnets $Dy_xY_{1-x}Al_2$

1994 J. Phys.: Condens. Matter 6 4779

(http://iopscience.iop.org/0953-8984/6/25/016)

J. Phys.: Condens. Matter 6 (1994) 4779–4794. Printed in the UK

Spin-glass behaviour in dilute weak random-anisotropy magnets $Dy_xY_{1-x}Al_2$

A del Moral†‡, J I Arnaudas† and P M Gehring‡§

† Laboratorio de Magnetismo, Departamento de Física de la Materia Condensada and Instituto de Ciencia de Materiales de Aragón, Universidad de Zaragoza and Consejo Superior de Investigaciones Científicas, 50009 Zaragoza, Spain

‡ Department of Physics and Materials Research Laboratory, 104 Goodwin Avenue, University of Illinois at Urbana-Champaign, IL 61801, USA

Received 9 August 1993, in final form 21 January 1994

Abstract. We have studied the magnetic phase diagram for the dilute alloys $(Dy_xY_{1-x})Al_2$ in the concentration range $0.10 \leqslant x \leqslant 0.50$. We find the systems to be disordered magnets with random magnetic anisotropy. For $x \leqslant 0.30$, the system undergoes a single transition from paramagnetic (PM) to spin-glass (SG) state. For $0.35 \leqslant x \leqslant 0.50$, a re-entrant coherent spin-glass (CSG) phase appears between the PM and SG states, formed by intrinsic nearly ferromagnetic domains. The triple point is located at $x \simeq 0.35$. However, no evidence of any long-range magnetic order was found in the concentration range studied. We have also determined the temperature variation of the spontaneous Edwards–Anderson order parameter for $x \leqslant 0.30$. The scaling analyses performed for the non-linear susceptibility indicate true phase transitions for the PM–SG line for $x < 0.35$, and yield values for the critical exponents β, γ and δ.

1. Introduction

In a previous publication [1] (paper I) we studied the static magnetic properties and critical behaviour of the series of pseudobinary intermetallics $Dy_xY_{1-x}Al_2$, and found them to be disordered magnets, presenting a weak random magnetic anisotropy (RMA), as a consequence of the dilution by yttrium. They crystallize in the Laves C-15 cubic structure, the Dy^{3+} and Y^{3+} ions randomly siting in a diamond lattice and the Al atoms forming a set of tetrahedra around the rare-earth (RE) lattice [2]. $DyAl_2$ is magnetically well characterized. It becomes a ferromagnet below $T_c \simeq 61.5$ K, according to low-field susceptibility, thermal expansion, coercive field, magnetocrystalline anisotropy and magnetostriction measurements [3–7], the easy magnetization axis being ⟨100⟩ [6, 8]. Anisotropy is large ($K_1 \simeq 36$ K/ion at 0 K) [5], although the quenching of Dy^{3+} magnetic moment by the crystal electric field (CEF) is small [9, 10]. YAl_2 is a Pauli paramagnet [11, 12]. In earlier studies [3, 5] of the magnetization mechanisms in the $Dy_xY_{1-x}Al_2$ series we concluded that, even for the 'concentrated' regime $x \geqslant 0.45$, the systems are magnetically imhomogeneous. We will discuss briefly why we expect these compounds to present RMA behaviour. First of all, the difference in lattice parameters between YAl_2 and $DyAl_2$ ($\simeq 0.37\%$) can give rise to an RMA energy contribution because of the large magnetoelastic coupling coefficient [7]. Moreover, the CEF screening is different for Y and Dy, which could imply a lowering of the otherwise

§ Present address: National Institute of Standards and Technology, Reactor Radiation Division, Gaithersburg, MD 20899, USA.

0953-8984/94/254779+16$19.50

local cubic symmetry. Finally the spin–orbit scattering strength is different for Y and Dy, and it can give rise, when RKKY (Ruderman–Kittel–Kasuya–Yoshida) exchange is present, to large off-diagonal Dzyaloshinsky–Moriya exchange interactions, contributing to the RMA effects.

The RMA systems have now been studied for over a decade [13–23]. Of paramount interest are the questions of whether or not a phase of infinite (or very large) susceptibility exists below some finite temperature T_c in an RMA system, biased by positive exchange interactions, and whether or not long-range magnetic order is precluded by the presence of RMA in Heisenberg-like systems. It was demonstrated by using several arguments and approximations [24, 25] that RMA destroys long-range magnetic order in less than four dimensions ($d < 4$). In fact, early theoretical developments [26, 27] demonstrated that a uniaxial RMA gives rise to an effective Hamiltonian of the same kind as that for random exchange systems with Ising symmetry. On the other hand, it is quite natural to expect that RMA might produce a spin-glass-like state, similar to the one induced by random exchange and frustration. However, in dealing with RMA systems one should distinguish between two situations, depending on the ratio between the exchange and RMA energies. At 0 K, when the ratio D_0/J_0 (where D_0 is the strength of the RMA CEF and J_0 is the average positive exchange interaction constant) is large (strong anisotropy), the system eventually evolves into single spins randomly frozen: the spin-glass (SG) phase. At the other extreme, for small D_0/J_0 values, the system will divide into quasiferromagnetic domains, becoming the so-called coherent or correlated spin-glass (CSG) system [28, 29]. Indeed, a crossover between the two phases can occur as the temperature increases and the ratio D_0/J_0 weakens [28].

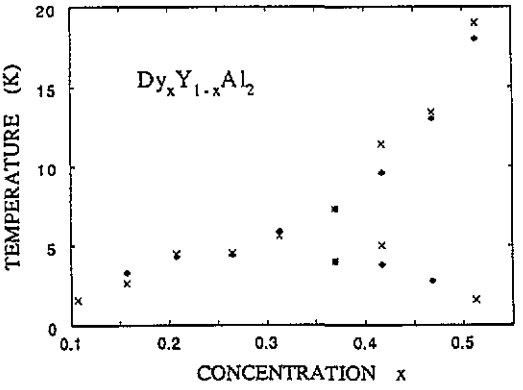

Figure 1. Magnetic phase diagram of the transition temperatures T_{SG} (P–SG transition) and T_c (CSG–SG transition) versus Dy^{3+} concentration x for $(Dy_xY_{1-x})Al_2$, obtained from SQUID-based DC magnetization measurements (×). The symbols ♦ denote the 'freezing' spin-glass temperatures (T_f) at $f = 15$ Hz, obtained from AC susceptibility measurements.

The above effects were observed in the present diluted compounds, because both the Dy concentration x and temperature affect D_0/J_0. For $x < 0.30$ the systems undergo a transition from paramagnetic (P) to SG state; however, for $0.30 < x \leqslant 0.50$, a CSG phase is re-entrant between the P and SG phases (see figure 1), the transition happening at temperatures $T_c(x)$. For the P–CSG transition, a ferromagnetic-like scaling analysis was performed, based on a modification of the equation of state for weak RMA systems proposed by Aharony and Pytte [30]. From the deduced critical exponents, only the pure $DyAl_2$ system can be classified as

a true ferromagnet. Further, we showed that for $x \simeq 0.62$ the system suffers a first-order magnetic phase transition to a quasi- or random-ferromagnetic state [31], with a crossover to a pure ferromagnetic state at $x = 0.87$. In the present work we have focused on the spin-glass behaviour in these alloys, which, to our knowledge, has never before been observed in *crystalline* Laves-phase compounds, although spin-glass order has been observed in the related amorphous alloys $GdAl_2$ [32], $(LaGd)Al_2$ [33] and $Ce(Fe_{0.8}Al_{0.2})_2$ [34].

2. Experimental details

The dilute $(Dy_xY_{1-x})Al_2$ alloys ($0.10 \leqslant x \leqslant 0.50$) were prepared by argon arc melting starting from Dy and Y of 99.9% and Al of 99.999% purities, respectively. The resulting buttons were remelted several times for homogeneity and annealed for one week at a temperature of 800 °C. The compound lattice parameters were determined from x-ray powder diffraction and were found to vary reasonably linearly with x (Vegard's law), with values in good agreement with those found in the literature [2] for pure $DyAl_2$ and YAl_2 (see figure 2). Metallographic analyses were also undertaken using optical and scanning electron microscopy (SEM) in the back-scattered electron (BSE) mode. A full account of this study may be found elsewhere [9, 10]. No evidence was found for a secondary phase in any of the samples reported in this paper. The actual sample concentrations (see table 1) were determined from a wavelength dispersive x-ray analysis, accurate to 2% [10]. Uniformity of the Dy dilution was checked through the variation of paramagnetic Curie temperatures with x (see [10] and paper I). For simplicity we will refer to the samples throughout this work by their nominal concentrations.

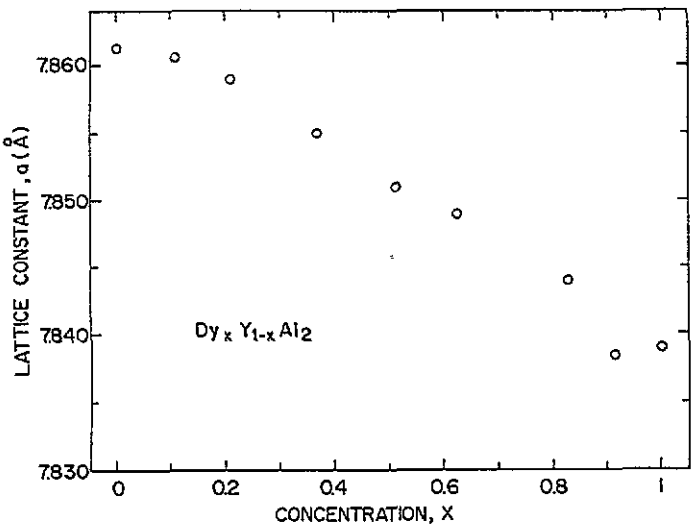

Figure 2. Dependence of the cubic lattice constant versus Dy concentration x for the $(Dy_xY_{1-x})Al_2$ series.

Two kinds of magnetic measurements were performed. DC magnetization measurements were carried out using a commercial SHE (S.H.E. Co., CA 92121, USA) VTS-50 SQUID (superconducting quantum interference device) magnetometer on polycrystalline,

rectangular-shaped samples about 3 mm and 6.5 mm in length and 1 mm square. The precision and stability of the temperature were roughly 0.01 K, and the accuracy of the measured moment was about 1 part in 10^4. Magnetic fields from 0 to 5 T were produced with a shielded, superconducting magnet. Great care had to be taken upon changing and latching a new field as the Nb_3Sn shield was prone to trapping substantial amounts of flux. Best results were obtained by latching a genuine zero field (obtained by heating the superconducting Nb_3Sn shield above its transition temperature, T_s, then fixing to zero value the solenoid current and finally cooling down the shield below T_s), and then setting subsequent fields in ascending order and taking data accordingly. When sufficient time was allowed for any residual supercurrents in the Nb_3Sn shield to decay (nominally 5 min), the accuracy in the field setting was generally 5% or better. For low-field measurements ($H_{app} \leqslant 1000$ Oe), an NBS magnetic-moment standard of Pd was used to calibrate the field.

Measurements were taken in a zero applied field, obtained and calibrated as indicated above, by cooling the sample to the lowest accessible temperature of $\simeq 1.6$ K and then measuring the magnetization while warming, applying a static magnetic field of 0.8 Oe. Data acquisition was fully automated on the SQUID magnetometer, and a total of 10 to 15 points were averaged to obtain the magnetization at a given temperature. In the study of high-susceptibility materials, which can be the situation here, demagnetizing effects must be treated carefully. The demagnetizing factor was estimated for each sample, the values ranging between 0.071 and 0.143.

The AC susceptibility measurements were performed using a modified Hartshorn mutual inductance bridge, working at a frequency of 15 Hz and a peak field value of roughly 35 mOe. Measurements were taken from $\simeq 2.2$ K up to well into the paramagnetic regime for each of the compounds with nominal Dy concentrations $x = 0.10$, 0.15, 0.20, 0.25, 0.30, 0.35, 0.40, 0.45 and 0.50. The measurement allows the determination of the real and imaginary parts of the AC susceptibility, χ'_{AC} and χ''_{AC}, respectively. These results are presented in section 4.1.

3. Theoretical background

We will briefly outline the theoretical results that are relevant to our measurements in the dilute $(Dy_xY_{1-x})Al_2$ magnets. As mentioned before, Aharony [26] considers a system described by the Hamiltonian

$$H = -\sum_{i,j} J_{ij} \boldsymbol{S}_i \cdot \boldsymbol{S}_j - D_0 \sum_i (\hat{\boldsymbol{a}}_i \cdot \boldsymbol{S}_i)^2 \tag{1}$$

where $\boldsymbol{S}_i$ is an m-component spin located at the ith site of a d-dimensional lattice, J_{ij} is the exchange interaction constant between spins i and j, and $\hat{\boldsymbol{a}}_i$ is a unit vector that randomly points in the direction of the magnetic anisotropy at site i, having fixed strength D_0. Using this Hamiltonian, Chen and Lubensky [27] (see also [35], which is a generalization of Chen and Lubensky's transition-temperature equation to high-spin RMA systems) showed that the system undergoes a spin-glass ordering transition at a temperature controlled by the anisotropy strength D_0, i.e. $T_{SG}^2 = D_0^2(1 - 1/m)/[m(m + 2)]$. The Hamiltonian (1) was transformed to a form identical to the one used by Sherrington and Kirkpatrick (SK) [36] for the random-exchange SG model, except that the *site* indices are replaced by spin *components* [35, 37]. Indeed, all of the results obtained in the SK model are translated to the RMA magnets, including the existence of a phase transition temperature. The only

significant difference is that now the Edwards–Anderson (EA) order parameter is defined in a slightly different form [35, 38], i.e. $q = (1/m)\sum_{j=1}^{m}\langle S_j^{\alpha} S_j^{\beta}\rangle_n$, where $\langle\ldots\rangle_n$ is an average over the n-replicas space.

Now, depending on the anisotropy-to-exchange ratio, RMA systems can sustain two kinds of magnetic ordering, as was noted in section 1. At low enough temperatures, $T < T_{SG}$, the anisotropy is strong and the system becomes an SG (or a speromagnet in Coey's nomenclature [14]). At higher temperatures, $T_{SG} < T < T_C$, the system becomes a CGS [28], where the spontaneous magnetization remains zero, but the system becomes divided into quasiferromagnetic intrinsic or Imry and Ma domains [39].

In the CSG state the local magnetization changes direction smoothly only over long distances $L \geqslant \xi_f$, the ferromagnetic correlation length. For $d = 3$, $\xi_f = \frac{15}{2}\xi_a(H_{ex}/H_r)^2$, where ξ_a is the distance over which the RMA local easy directions are correlated, and H_{ex} and H_r are the effective exchange and anisotropy fields, respectively. The crossover from weak ($\xi_f \gg \xi_a$) to strong ($\xi_f \simeq \xi_a$) RMA is determined by the criterion $H_r/H_{ex} = (H_r/H_{ex})_{crit} \simeq 1$–3. This opens the possibility [28] of a re-entrant SG phase in some range of Dy^{3+} concentration. For single-ion anisotropy, the RMA strength $\beta_r \equiv H_r/M_0$ depends strongly upon T but weakly upon x, while the exchange stiffness $\alpha \equiv (H_{ex}/M_0)\xi_a^2$ should be independent of T, but increases with increasing x. Therefore the condition for re-entrance [28] should be $H_r[T_{SG}(x)]/H_{ex}(x) \simeq (H_r/H_{ex})_{crit}$. It is clear from this expression that, as x increases (so that H_{ex} also increases), so does $H_r[T_{SG}]$. We believe that re-entrance has been observed in the $(Dy_xY_{1-x})Al_2$ systems (see figure 1 and table 1).

We will next consider some aspects related to the scaling behaviour. Given the strong similarities between random-exchange spin glasses and RMA systems, the scaling results of Suzuki *et al* [40, 41] for the SG non-linear susceptibility are likely to be applicable to the present system. If one defines the non-linear susceptibility in the usual way as $\chi_{nl} = (M/H) - (M/H)_{H\to 0} \equiv \chi - \chi_0$, then it is easy to deduce [40, 41] the following scaling form for χ_{nl},

$$\chi_{nl} = t^{\beta} f(H^2/t^{\gamma+\beta}). \tag{2}$$

Equation (2) can be written in the equivalent form $\chi_{nl} = H^{2/\delta} g(t/H^{2/\phi})$, by using the scaling relations $\phi = \beta + \gamma$ and $\beta = \phi/\delta$. From the previous expressions it follows [42, 43] that $\chi_{nl} \sim H^2 t^{-\gamma}$, for $t > 0$ and small H, and $\chi_{nl} \sim H^{2/\delta}$, for $T = T_{SG}$.

Let us consider now the initial susceptibility and the spin-glass order parameter. The low static magnetic field susceptibility, χ_0, is a simple probe with which to determine the local magnetic SG order parameter [32, 44]. In fact, when magnetic interactions are present, the Fischer [44] equation in a finite applied magnetic field can be written as

$$M/H \equiv \chi = C(1-q)/[T - \theta(1-q)] \tag{3}$$

where C is the Curie constant, which, for a rare-earth system, is

$$C = (N/3k_B)[(g-1)\mu_B]^2 J(J+1). \tag{4}$$

Here N is the number of RE ions per unit volume and $\theta \simeq N(J_0/k_B)$ is the paramagnetic Curie temperature. Also, in equation (3), q must be replaced by $q^* \equiv q/(g-1)^2 J(J+1)$. It is important for the following discussion to recognize that the EA order parameter q and the non-linear susceptibility are proportional [40, 45], i.e.

$$\chi_{nl} \equiv -\chi_{00} q \tag{5}$$

where $\chi_{00} = C/T$ is the regular Curie paramagnetic susceptibility. For low enough values of the argument, we can expand $f(x)$ in equation (2). Keeping only the first two terms in the expansion and using equation (5), we obtain

$$q = -[f(0)/\chi_{00}]t^{\beta} - [f'(0)/\chi_{00}]H^2 t^{-\gamma} + \cdots. \tag{6}$$

This is a strong indication that q contains a spontaneous part, q_{sp} (for $H = 0$), and a divergent singular one, q_{sing}. We have, from (5) and (3), neglecting the θ term in equation (3) for now,

$$\chi \simeq \chi_{00}[1 - (q_{sp} - q_{sing})]. \tag{7}$$

Then, because $q_{sing} = 0$ as $H \to 0$, the measurement of the *initial* susceptibility yields the *spontaneous* SG order parameter below T_{SG} [32, 46].

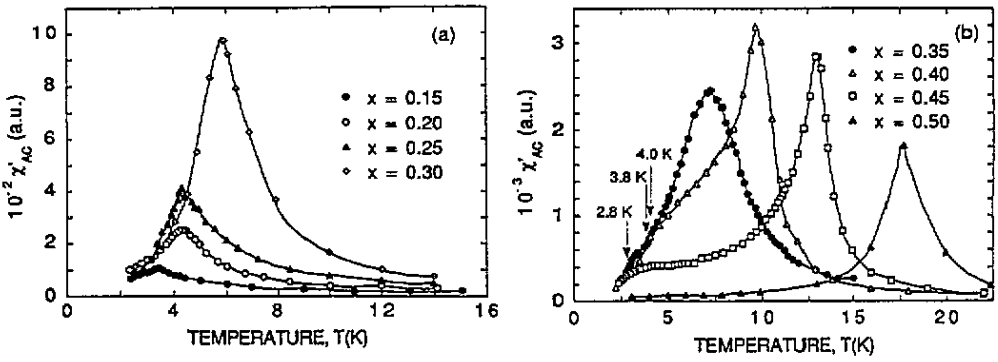

Figure 3. Thermal variation of the real part of the initial AC susceptibility χ'_{AC}, measured in an applied AC field of 35 mOe peak value at a frequency of 15 Hz (in (*b*) the arrows indicate the CSG–SG 'freezing' temperatures, T_f; see table 1 and section 4.1 for details).

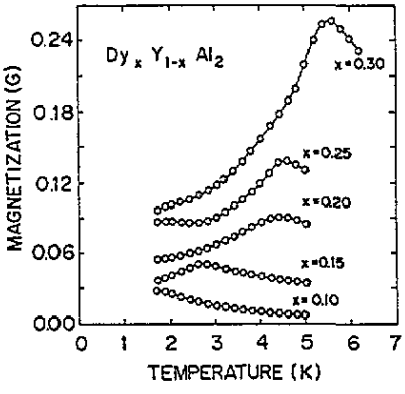

Figure 4. Zero-field cooled DC magnetization versus temperature, measured in an applied field of 0.8 Oe, for Dy concentrations $x \leqslant 0.30$. Curves have been offset for clarity, but the relative sizes have been preserved.

Table 1. 'Freezing' spin-glass temperatures for an AC measuring low magnetic field of frequency 15 Hz (T_f), spin-glass transition temperatures (T_{SG}) and paramagnetic Curie temperatures (θ) for the diluted $Dy_xY_{1-x}Al_2$ intermetallic compounds. Also quoted are the critical exponent values for the Edwards–Anderson order parameter q^* (see section 4.2 for details).

Concentration x		T_f[a]	T_{SG}[b]	θ	
nominal	real	(K)	(K)	(K)	β
0.10	0.107	—	1.58	—	—
0.15	0.157	3.3	2.64	1.8 ± 0.1	1.1
0.20	0.208	4.3	4.46	2.3 ± 0.5	1.1
0.25	0.265	4.4	4.51	2.4 ± 0.5	1.1
0.30	0.313	5.9	5.60	4.4 ± 0.3	1.1
0.35	0.370	4.0	4.00	—	—
0.40	0.417	3.8	5.00	—	—
0.45	0.468	2.8	—	—	—
0.50	0.517	—	1.6	—	—

[a] From AC susceptibility measurements (this work).
[b] From DC magnetization measurements (this work and [1]).

4. Experimental results and discussion

4.1. Low-field AC susceptibility, transition temperatures and phase diagram

We have plotted the real part of the AC susceptibility, χ'_{AC}, versus temperature in figures 3(a) and (b) for $0.15 \leqslant x \leqslant 0.50$ in the $(Dy_xY_{1-x})Al_2$ system. For $x \leqslant 0.30$, maxima are observed at temperatures T_f, which we identify with the slow 'freezing' of the spins at the measurement frequency of 15 Hz. The zero-field cooled (ZFC) DC magnetization measurements also display broad maxima at temperatures T_{SG} close to the corresponding T_f values (see figure 4 and table 1). We should expect values of T_{SG} smaller than T_f, as should happen for static and dynamic magnetization measurements, but the small differences observed between them are not always of the same sign, and therefore they should not be ascribed to the above expectation. Such differences are probably due to thermometry effects for the different experimental set-ups. For $x > 0.30$ (figure 3(b)), the first peak in the AC susceptibility measurements develops into an elbow, and a second peak appears, which we identify with the PM–CSG transition temperature T_c. For concentrations $x \leqslant 0.30$, a thermal irreversibility was observed starting at T_{SG} between the ZFC isofields and the isofields measured cooling in field (FC).

Based on all these results, the magnetic phase diagram was derived (see figure 1). Below the PM–SG line the system is in a spin-glass state; above the triple point $x = 0.30$ the SG is re-entrant into a CSG state, below the SG–CSG line. As expected theoretically (see section 3), above the triple point $x = 0.30$, T_{SG} in fact decreases as x increases.

Further evidence is gained from the imaginary component of the initial AC susceptibility, χ''_{AC}, which is plotted in figures 5(a) and (b). For $x \leqslant 0.30$, weak but well defined peaks are observed at slightly lower temperatures than those for χ'_{AC}, the maximum of χ''_{AC} coinciding with the inflection point of χ'_{AC}. For $x \geqslant 0.35$ the SG–CSG transitions are now better defined than in figure 3(b) through the shoulders ($x = 0.35$, 0.40) and peak ($x = 0.45$) appearing at temperatures where the shoulders of χ'_{AC} change more rapidly. Such features have been seen in other spin-glass systems [47, 48].

4.2. Low- and high-field magnetization: spin-glass order parameter and transition lines

4.2.1. Spin-glass order parameter. We have used equation (3) and χ_0, obtained from the

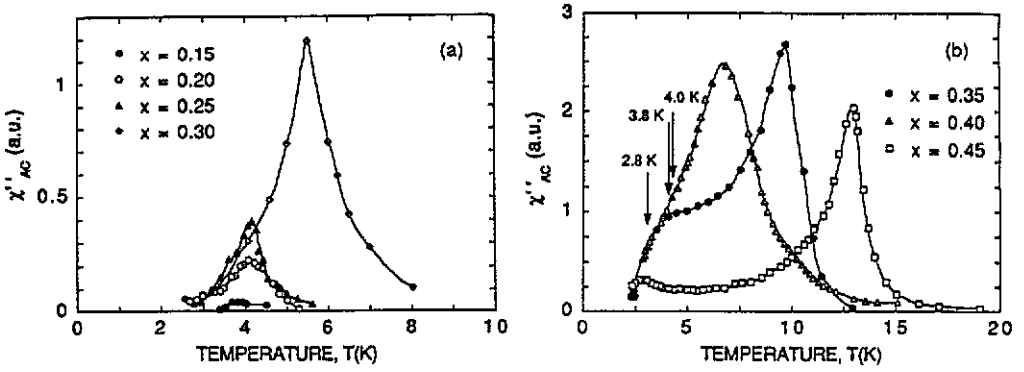

Figure 5. Same as figure 3 for the imaginary part of the initial AC susceptibility χ''_{AC}.

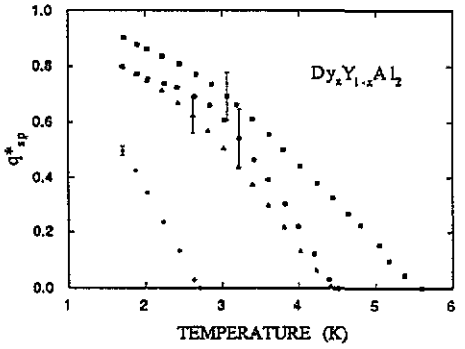

Figure 6. Thermal dependence of the reduced spontaneous spin-glass order parameter q^*_{sp} below the PM–SG transition temperature T_{SG}, determined at an applied field of 0.8 Oe, for $x = 0.15$ (♦), 0.20 (▲), 0.25 (●) and 0.30 (■). The error bars represent the uncertainty introduced by the uncertainty in the determined paramagnetic Curie temperature θ values (see table 1 and section 4.2 for details).

low-field DC magnetization measurements (figure 4), to determine the thermal variation of the spin-glass order parameter q^* for the different $(Dy_xY_{1-x})Al_2$ compounds, as shown in figure 6. For the compounds with $x < 0.35$, the CSG phase is not present, and the determination of the paramagnetic temperature, θ, by extrapolation of $1/\chi'_{AC}$ down to zero is quite straightforward. However, in order to obtain a reasonable temperature variation for q^* it is necessary to extrapolate in the region near T_{SG} due to the strong curvature of $1/\chi'_{AC}$ near T_f [46]. In figure 7 we show the plots of $1/\chi'_{AC}$ versus temperature, the straight lines indicating how the θ values were obtained. We should mention that such curvature is usually ascribed to clustering behaviour, as we show that it happens, in section 4.2.2. below. The values of θ are *positive* for all concentrations, indicating a dominant ferromagnetic exchange interaction, as assumed in section 3. The linearity of the plots in figure 6, close to T_{SG}, indicates that $\beta \gtrsim 1$, as also shown by the scaling $q \sim t^{\beta}$, according to equation (6) for $H \to 0$. Inasmuch that χ_0 was obtained at an applied field of 0.8 Oe, the scaled q parameter should be fairly close to q_{sp}. In fact the β values so obtained (see table 1) are in fair agreement with the values obtained below from the non-linear susceptibility. These results lend strong support to the claim that the PM–SG transition for $x \leqslant 0.30$ is indeed a

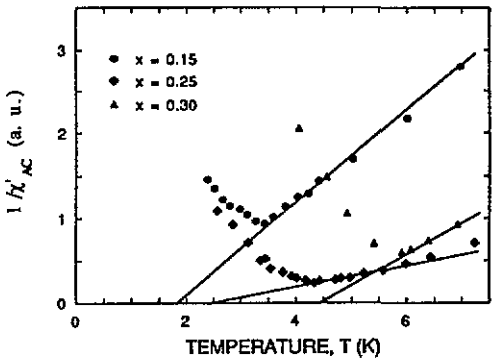

Figure 7. The inverse susceptibility $1/\chi'_{AC}$ against temperature for the $(Dy_xY_{1-x})Al_2$ alloys. Also shown are the linear extrapolations of $1/\chi'_{AC}$ near T_f (full lines) in order to determine the paramagnetic Curie temperature θ values, from the x-axis intercepts.

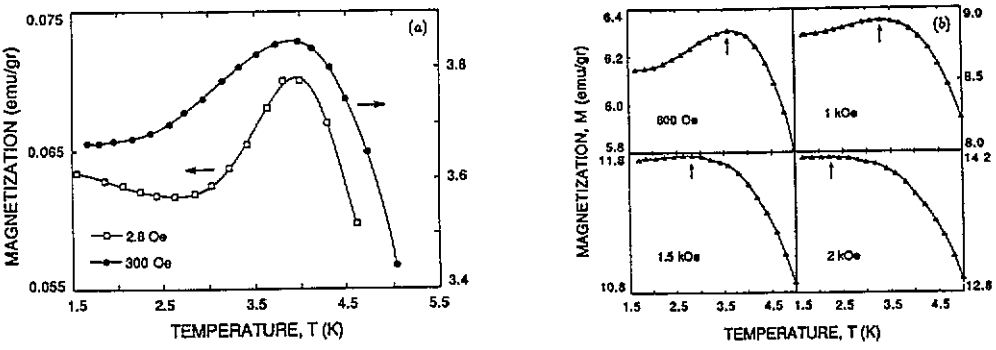

Figure 8. Thermal variation of the magnetization in increasing magnetic fields (2.8 Oe $\leqslant H \leqslant$ 2 kOe) for the compound $(Dy_{0.20}Y_{0.80})Al_2$. The wide cusps signal the onset of the SG phase.

true phase transition.

4.2.2. Transition lines. SQUID-based DC magnetization measurements were performed at several fields from $\simeq$ 1 Oe to 5 kOe at temperatures from 1.7 K to well into the paramagnetic region. In the concentration range $0.10 \leqslant x \leqslant 0.30$, the magnetization at low fields shows a broad maximum around T_{SG}, which shifts towards lower temperatures as the field increases (see figures 8(a) and (b) for the compound $x = 0.20$). The SG transition lines are of the Gabay–Toulouse (GT) type, i.e. being fitted by the law $H = H_{GT}[1 - T(H)/T_{SG}]^{1/2}$ [49], obtaining from the fits the values $H_{GT} = 2.4 \pm 0.1$ and 2.3 ± 0.1 kOe for $x = 0.20$ and 0.30, respectively, indicating a Heisenberg character for our systems. At this point, it is interesting to speculate on whether or not clustering in these systems might be inferred from the value of H_{GT}. The MFA gives the result [48]

$$\mu_{cluster}H_{GT} = \left(\frac{4(m+2)^2}{m^2+4m+2}\right)^{1/2} k_B T_{SG}. \tag{8}$$

By using the previous values for H_{GT} one obtains $57\mu_B$ and $74\mu_B$ per $\mu_{cluster}$ for $x = 0.20$ and 0.30, respectively, which suggests a small amount of clustering since the Dy moment

is $10\mu_B$. As we said in section 4.2.1, this result fits in well with the curvature of $1/\chi'_{AC}$ near T_{SG}.

4.3. Arrot plots

For RMA systems the initial susceptibility $\chi_0 \equiv (M/H)_{H\to 0}$ must approach a limiting value $\propto (J_0/D_0)^4$ [28, 50] below the transition temperature T_{SG}, or diverge (as in the case where $D_0 \to 0$). In practice, however, the experimental susceptibility must be limited by the demagnetizing factor N, i.e.

$$1/\chi_{exp} = 1/\chi_0 + 4\pi N. \tag{9}$$

The divergence of χ_0 follows from an equation of state derived by Aharony and Pytte [30] for weak RMA systems.

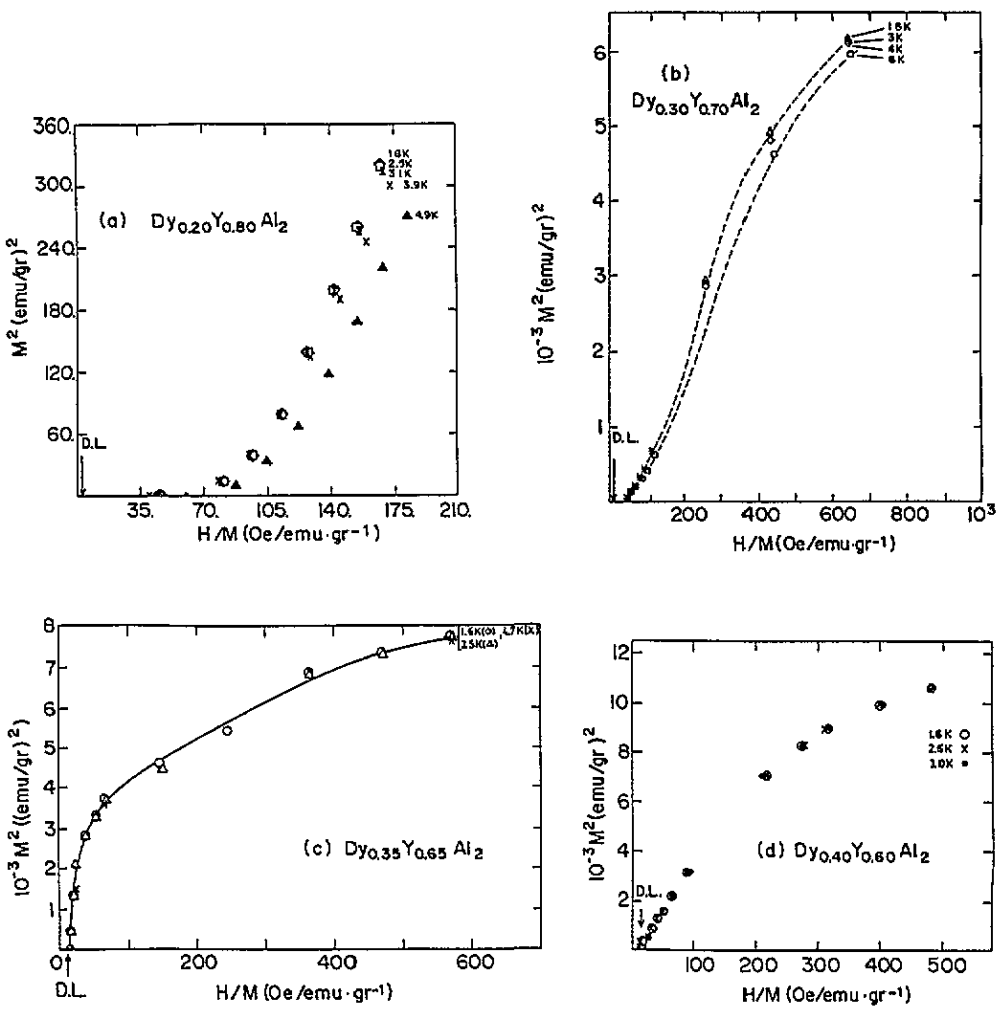

Figure 9. Arrott plots of M^2 versus H/M for $x = 0.20$, 0.30, 0.35 and 0.40 compounds (DL denotes the expected demagnetization limit values for H/M).

To test these predictions we have made Arrott plots in the usual form of M^2 versus H/M at the SG phase, as shown in figures 9(*a*)–(*d*). We can see that for the higher concentrations, $x \geqslant 0.35$, χ_0 reaches the demagnetizing limit, but it does not for the lower concentrations. In addition, we note that the downwards curvature of the Arrott plots for concentrations $x = 0.35$ and 0.40 is in agreement with the predicted one by Aharony and Pytte [30] for weak RMA systems. Instead the curvature is the opposite for the lower concentrations. This seems to indicate a continuous decrease of D_0/J_0 with Dy content.

4.4. Non-linear susceptibility

Because the effective Hamiltonian for strong enough RMA systems is formally identical to that for the case of random exchange, they should behave as spin glasses below the CSG–SG or PM–SG transition lines. Thus, according to scaling theory [40], it is the non-linear susceptibility χ_{nl} that should exhibit critical behaviour near T_{SG} (see section 3) (a preliminary study of χ_{nl} for the present systems was published elsewhere [51]). We have arbitrarily taken for χ_0 the values obtained at the lowest field measured, great care being exercised in correcting the field values for remanence effects in the SQUID superconducting coil (see also section 2). The fields used to obtain χ_0 respectively were: 1.8 and 2.13 Oe for the $x = 0.20$ and 0.30 compounds. In figure 10 we show the thermal variation of χ_{nl} for the $x = 0.30$ compound in increasing magnetic field. There is no shift of the maxima with field; inasmuch as χ_{nl} is the effective order parameter in SG systems, according to equation (5), the maximum of χ_{nl} signals the transition temperature T_{SG}.

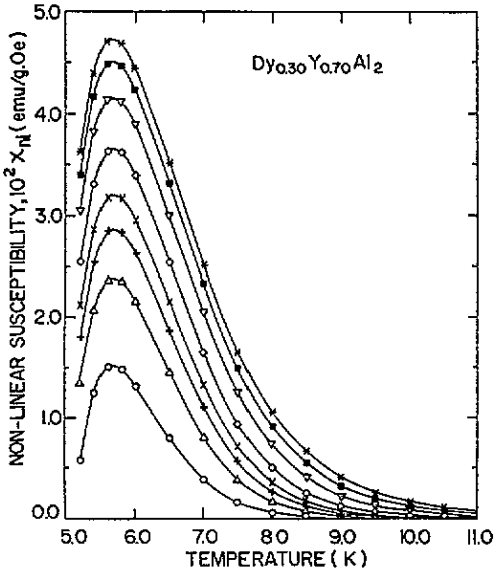

Figure 10. Non-linear susceptibility for $(Dy_{0.30}Y_{0.70})Al_2$. The linear susceptibility used to compute the non-linear susceptibility was taken in a field of 2.13 Oe The data, from the lowest to the highest curves, were taken in successively increasing fields of 42, 92, 142, 192, 292, 492, 742 and 992 Oe.

We will now turn our attention to the scaling behaviour of χ_{nl} with field. Plotting χ_{nl} versus H as done in figure 11 (see section 3), we can extract the values $\delta = 4.5$ and 4.4

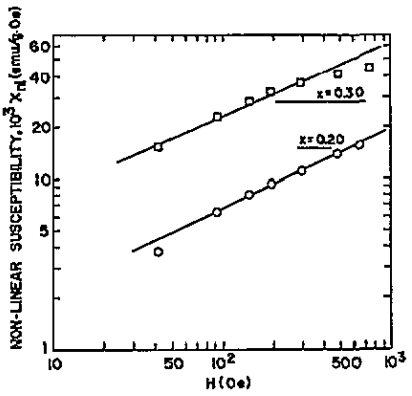

Figure 11. Critical scaling of χ_{nl} versus $H^{2/\delta}$ at $T = T_{SG}$ for $x = 0.20$ and $x = 0.30$. The slopes of the lines give $2/\delta$, with $\delta = 4.4$ ($x = 0.20$) and 4.5 ($x = 0.30$).

Table 2. Critical exponents in some dilute $Dy_xY_{1-x}Al_2$ alloys for the non-linear susceptibility.

x	β	δ	γ
0.208	—	4.4[a]	—
	1.3[b]	4.4[b]	4.4[c]
0.313	—	4.5[a]	—
	1.3[b]	4.4[b]	4.4[c]

[a] Obtained from $\chi_{nl} \sim H^{2/\delta}$ scaling plots.
[b] Obtained from χ_{nl}/t^{β} versus $H/t^{\beta\delta/2}$ scaling plots.
[c] Obtained from the scaling relation $\gamma = \beta(\delta - 1)$.

for $x = 0.30$ and 0.20 respectively. The plot is fairly linear for low fields ($H \leqslant 700$ Oe), but our estimated values for δ are somewhat larger than the values for other spin glasses (see table 2), although large values have been observed in several SG systems such as a-$GdAl_2$ ($\delta = 6.1$) and $CuMn_{1\ at.\%}$ ($\delta = 5.7$) [20, 52]. We have also performed a scaling analysis of the form suggested by equation (2). In figures 12(*a*) and (*b*), we plot, in double-logarithmic scales, $\chi_{nl}/|t|^{\beta}$ versus $H/|t|^{\beta\delta/2}$, for the $x = 0.20$ and 0.30 compounds, where $t = (T_{SG} - T)/T_{SG}$, the values used for T_{SG} being given in table 1. The critical exponents obtained from the best collapse of the data points are displayed in table 2. The agreement with the values directly determined is reasonably good. On the same plots are shown the lines of H^2 and $H^{2/\delta}$ for the $t > 0$ and $t = 0$ isotherms.

4.5. Critical relaxation time

At the phase transition from paramagnetic to SG, the system should suffer critical slowing down when the transition temperature is approached from above. Any relaxation or response time should diverge as [53] $\tau \propto t^{-z\nu}$, where z is the dynamic critical exponent and ν is the correlation length critical exponent.

In order to investigate the critical slowing down in spin glasses, where a broad spectrum of relaxation times seems to exist, even at the paramagnetic regime, we can consider the expressions of $\chi'(\omega)$ and $\chi''(\omega)$ within the Debye approximation, valid for an SG at the *paramagnetic* regime [54], i.e.

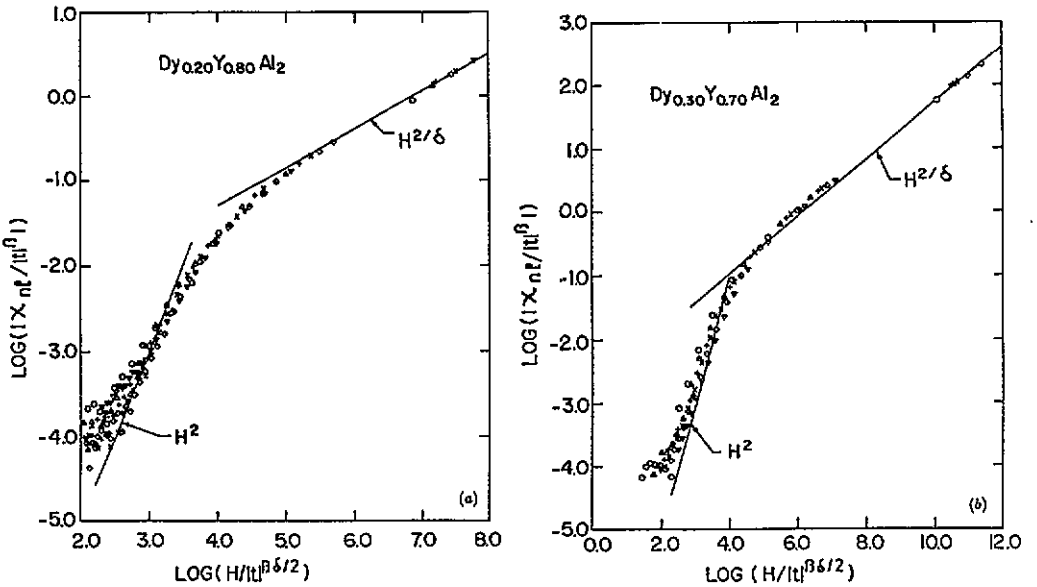

Figure 12. (*a*) Scaled non-linear susceptibility χ_{nl}/t^{β} of $(Dy_{0.20}Y_{0.80})Al_2$ versus the scaled magnetic field $H/t^{\beta\delta/2}$, where $t = (T - T_{SG})/T_{SG}$. The determined critical exponents and T_{SG} values giving the best 'collapse' of the data points are $\beta = 1.3$, $\delta = 4.4$ and $T_{SG} = 4.46$ K, respectively. The full lines give the expected asymptotic slopes of the scaling function. Data in fields < 500 Oe and $T > T_{SG}$ are included. (*b*) The same plot for $(Dy_{0.30}Y_{0.70})Al_2$, using the same exponents, with $T_{SG} = 5.60$ K.

$$\chi' = \frac{1}{H}\int_0^{\infty} \frac{M(\tau)\rho(\tau)}{(1+\omega^2\tau^2)}\,d\tau$$

$$\chi'' = \frac{1}{H}\int_0^{\infty} \frac{M(\tau)\rho(\tau)\omega\tau}{(1+\omega^2\tau^2)}\,d\tau \qquad (10)$$

where $\rho(\tau)$ is the relaxation time, τ is the distribution function and ω is the measuring AC magnetic-field frequency. In the case of having a system with a single relaxation time, the experimentally determinable quantity $\chi''/\omega\chi'$ directly lends the value of such a time. However if, as in our case, we have a time distribution $\rho(\tau)$, we can only write

$$\chi''(\omega)/\omega\chi'(\omega) = \bar{\tau} \qquad (11)$$

where $\bar{\tau}$ is certainly a relaxation time but, being frequency-dependent, is not a feature fully characteristic of the SG system. Only if we are within the regime $\omega\tau \ll 1$ does $\bar{\tau}$ represent a true characteristic or average time [55] of the system, i.e. ω-independent, as can be immediately verified from equation (10). Now, if we apply equation (11) to our AC susceptibility results, taken at the fixed frequency $\omega/2\pi = 15$ Hz, we will obtain some characteristic average relaxation time only if the above $\omega\tau \ll 1$ condition is fulfilled, for instance for times $\tau < 10^{-2}/\omega$ (a thorough study of the distribution of relaxation times could have been performed by measuring $\chi'(\omega, T)$ and $\chi''(\omega, T)$ at variable frequency, but this is not feasible with our experimental set-up). Although we are aware that such an average time is not fully representative of all the relaxation times of the spectrum of the

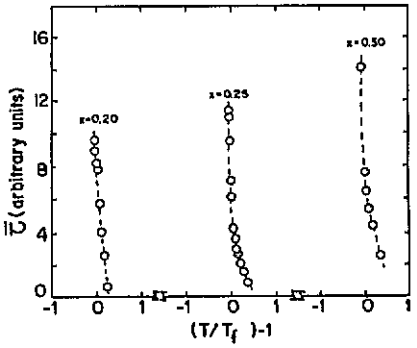

Figure 13. Thermal variation of the average relaxation time $\bar{\tau}$ (see meaning in text), near and above the PM–SG transition temperature, T_{SG}, for $x = 0.20$, 0.25 and 0.30. The lines are guides to the eye.

system, nevertheless we have plotted its thermal variation (see figure 13) for the compounds suffering a PM–SG transition. The observed very rapid increase of $\bar{\tau}$ on approaching T_f from above agrees well with the above proved phase transitions at T_{SG}, and gives us additional information, although only qualitative, about the existence of those phase transitions.

5. Conclusions

We conclude from our magnetic measurements that the *crystalline* $(Dy_xY_{1-x})Al_2$ pseudobinary intermetallic compounds are disordered magnetic systems possessing random magnetic anisotropy. The magnetic phase diagram has been determined and shows that for $x > 0.35$ the system presents two magnetic phases, a high-temperature correlated spin-glass phase, and a spin-glass phase at the lowest temperatures, $x \simeq 0.35$ being the triple point. For concentrations $x \leqslant 0.313$, we have shown that a true phase transition from paramagnetic to spin glass does exist. Besides, the existence of a Gabay–Toulouse line, for $x \leqslant 0.313$, on crossing from paramagnetic to SG phase, points to a Heisenberg character for our systems.

From the Arrott plots we have shown that no long-range magnetic order appears in any of the systems studied, and also that the ratio D_0/J_0, between the RMA CEF strength and the exchange strength, should decrease with the Dy content.

From the low-field DC susceptibility and using the Fischer formula [44], considering the presence of positive exchange interactions, we have been able to determine the temperature variation of the *spontaneous* Edwards–Anderson order parameter, which shows a β exponent of 1.1, close to the theoretical MFA prediction ($\beta = 1$) [40].

The non-lineaer susceptibility, χ_{nl}, for these RMA systems should behave as it does in the case of random exchange spin glasses, inasmuch as both cases are described by formally equivalent effective Hamiltonians. In fact we find that χ_{nl} scales as $\chi_{nl} = t^{-\beta} f(H^2/t^{\beta\delta})$, thereby showing critical behaviour. Somewhat larger values are obtained for the exponent δ, which governs the field scaling behaviour of χ_{nl}. However, large values for δ have also been found for other archetypal spin glasses and in amorphous RMA systems. The critical exponents so determined, β, δ and γ, are summarized in table 2.

Acknowledgments

We acknowledge financial support from the Spanish DGICYT under Grant PB 90/1014, from

the American NSF MRL Program DMR-8612860 and from the USA–Spain Joint Committee for Scientific and Technological Cooperation (Ref. ESB-8512017). We acknowledge very helpful experimental collaboration and discussions with Professor M B Salamon. We are also indebted to Professor J Tejada for allowing us to perform some of the SQUID-based magnetization measurements at the University of Barcelona. Useful discussions with Professor E Fradkin and Dr P Goldbart (University of Illinois at Urbana-Champaign) are also acknowledged.

References

[1] Gehring P M, del Moral A, Arnaudas J I and Salamon M B 1990 *Phys. Rev.* B **41** 9134
[2] Buschow K H J 1979 *Rep. Prog. Phys.* **42** 1373
[3] del Moral A and Arnaudas J I 1986 *J. Magn. Magn. Mater.* **62** 71
[4] Ibarra M R, Lee E W and del Moral A 1986 *Solid State Commun.* **57** 695
[5] Arnaudas J I, del Moral A and Abell J S 1986 *J. Magn. Magn. Mater.* **61** 370
[6] del Moral A, Ibarra M R, Abell J S and Montenegro J F D 1987 *Phys. Rev.* B **35** 6800
[7] Ibarra M R, Lee E W, del Moral A and Abell J S 1986 *J. Magn. Magn. Mater.* **54–57** 882
[8] Barbara B, Rossignol M F, Purwins M G and Walker E 1977 *Crystal Field Effects in Metals and Alloys* ed A Furrer (New York: Plenum) p 148
[9] Arnaudas J I 1985 *PhD Thesis* University of Zaragoza (unpublished)
[10] Gehring P M 1989 *PhD Thesis* University of Illinois, Urbana (unpublished)
[11] Williams H J, Wernick J H, Nesbitt E A and Sherwood R C 1962 *J. Phys. Soc. Japan* **17** Suppl. B-I, 91
[12] Buschow K H J, Fast J F, von Diepen A M and de Wijn H W 1967 *Phys. Status Solidi* **24** 715
[13] Harris R, Plischke M and Zuchermann M J 1973 *Phys. Rev. Lett.* **31** 160
[14] Coey J M D 1978 *J. Appl. Phys.* **49** 1646
[15] Rhyne J J, Schelleng J H and Koon N C 1974 *Phys. Rev.* B **11** 4672
[16] Barton L S and Salamon M B 1982 *Phys. Rev.* B **25** 2030
[17] von Molnar S, McGuire T R, Gambino R J and Barbara B 1982 *J. Appl. Phys.* **53** 7666
[18] von Molnar S, Barbara B, McGuire T R and Gambino R J 1982 *J. Appl. Phys.* **53** 2350
[19] Dieny B and Barbara B 1985 *J. Physique* **46** 293
[20] Dieny B and Barbara B 1986 *Phys. Rev. Lett.* **57** 1169
[21] Sellmyer D J and Nafis S 1986 *Phys. Rev. Lett.* **57** 1173
[22] Sellmyer D J and Nafis S 1986 *J. Magn. Magn. Mater.* **54–57** 113
[23] Imry Y and Ma S K 1975 *Phys. Rev. Lett.* **35** 1399
[24] Pelcovits R A, Pytte E and Rudnick J 1978 *Phys. Rev. Lett.* **40** 476
[25] Fischer K H and Zippelius A 1986 *Prog. Theor. Phys.* **87** Suppl., 165
del Moral A and Cullen J 1994 *J. Magn. Magn. Mater.* submitted
[26] Aharony A 1975 *Phys. Rev.* B **12** 1038
[27] Chen J H and Lubensky T C 1977 *Phys. Rev.* B **16** 2106
[28] Chudnovsky E M, Saslow W M and Serota R A 1986 *Phys. Rev.* B **33** 251
[29] Chudnovsky E M and Serota R A 1983 *J. Phys. C: Solid State Phys.* **16** 4181
[30] Aharony A and Pytte E 1980 *Phys. Rev. Lett.* **45** 1583
[31] del Moral A, Arnaudas J I, Gehring P M, Salamon M B, Ritter C, Joven E and Cullen J 1993 *Phys. Rev.* B **47** 7829
[32] Mizoguchi T, McGuire T R, Kirkpatrick S and Gambino R J 1977 *Phys. Rev. Lett.* **38** 89
[33] Bredl C D, Steglich F, Löhneysen H V and Matho K 1978 *J. Physique Coll.* **39** C6 925
[34] da Cunha S F, Franceschini P F, Senoussi S and Takeuchi A Y 1982 *J. Phys. F: Met. Phys.* **12** 3083
[35] del Moral A and Arnaudas J I 1989 *Phys. Rev.* B **39** 9453
[36] Sherrington D and Kirkpatrick S 1975 *Phys. Rev. Lett.* **35** 1792
[37] del Moral A and Arnaudas J I 1987 *Magnetic Properties of Amorphous Metals* ed A Hernando *et al* (Amsterdam: Elsevier) p 330
[38] Harris A B, Lubensky T C and Chen J H 1976 *Phys. Rev. Lett.* **36** 415
[39] Fischer K H 1987 *Phys. Rev.* B **36** 6963
[40] Suzuki M 1977 *Prog. Theor. Phys.* **58** 1151
[41] Katori M and Suzuki M 1985 *Prog. Theor. Phys.* **74** 1175
[42] Barbara B, Malozemoff A P and Barnes S E 1984 *J. Appl. Phys.* **55** 1655

[43] Malozemoff A P, Barnes S E and Barbara B 1983 *Phys. Rev. Lett.* **18** 1704
[44] Fischer K H 1975 *Phys. Rev. Lett.* **34** 1438
[45] Suzuki M and Miyashita S 1981 *Physica* **106A** 344
[46] del Moral A, Arnaudas J I and Mohammed K A 1986 *Solid State Commun.* **58** 395
[47] Goldfarb R G, Fickett F R, Rao K V and Chen H S 1982 *J. Appl. Phys.* **53** 7687
[48] Dormann J L, Snifi A, Cagan V and Nogues M 1985 *Phys. Status Solidi* b **131** 573
[49] Toulouse G and Gabay M 1981 *J. Physique Lett.* **42** L103
[50] Aharony A and Pytte E 1983 *Phys. Rev.* B **27** 5872
[51] del Moral A, Gehring P M, Arnaudas J I and Salamon M B 1988 *J. Physique Coll.* **49** C8, 1233
[52] Barbara B, Malozemoff A P and Imry Y 1982 *Phys. Rev. Lett.* **47** 1852
[53] Bontemps N, Rajchenbach J, Chamberlin R V and Orbach R 1984 *Phys. Rev.* B **30** 6514
[54] Lundgren L, Svedlinh P and Bechman O 1981 *J. Magn. Magn. Mater.* **25** 33
[55] Ogielsky A T 1985 *Phys. Rev.* B **32** 7384